# Geometric Wavelet Approximations and Differencing

Abdourrahmane Atto, Emmanuel Trouvé, Jean-Marie Nicolas

▶ **To cite this version:**

Abdourrahmane Atto, Emmanuel Trouvé, Jean-Marie Nicolas. Geometric Wavelet Approximations and Differencing. 2014. hal-00950823v1

**HAL Id: hal-00950823**

**https://hal.science/hal-00950823v1**

Preprint submitted on 22 Feb 2014 (v1), last revised 26 Jan 2016 (v3)

**HAL** is a multi-disciplinary open access archive for the deposit and dissemination of scientific research documents, whether they are published or not. The documents may come from teaching and research institutions in France or abroad, or from public or private research centers.

L'archive ouverte pluridisciplinaire **HAL**, est destinée au dépôt et à la diffusion de documents scientifiques de niveau recherche, publiés ou non, émanant des établissements d'enseignement et de recherche français ou étrangers, des laboratoires publics ou privés.

# Geometric Wavelet Approximations and Differencing

Abdourrahmane M. Atto[1], Emmanuel Trouvé[2] Jean-Marie Nicolas[3],

***Abstract*—The paper introduces the concept of geometric wavelets defined from multiplicative algebras. These wavelets perform generalized geometric approximations and differencing. The paper also highlights the statistical properties of multiplicative observation models when the analysis is performed by using multiplicative wavelet transforms. It shows that multiplicative wavelets are more relevant for the representation of piecewise smooth signals observed in presence of multiplicative noise, the sole case where additive and multiplicative wavelet transforms share the same properties being the case of constant signals.**

***Index Terms*—Wavelets ; Geometric convolution ;Geometric approximations ; Geometric differencing.**

## I. Introduction - Motivation

HIGHLY resolved data such as signals and images issued from modern sensors exhibit sharp details. As a consequence, these data make non-valid, the standard assumption consisting in liken as constant, the focuses on tiny signal parts or small image patchs. This compels us for re-considering data representations and processing principles.

In this paper, we focus on data associated with multiplicative type interactions. Those data are observed in many situations, for instance when acquiring signals from radar/sonar/ultrasonic waves [1]/[2]/[3],[4], when analyzing seasonality from meteorology data [5] or when focusing on proportionality in economy data [6] and political sciences [7].

A multiplicative observation model involving strictly positive interactions of a piecewise regular function $\mathrm{f}$ and a random noise $\mathrm{X}$ can be written as:

$$\mathbf{y} = \mathrm{f}\mathbf{X} = \mathrm{f} + \mathrm{f}(\mathbf{X} - 1) \qquad (1)$$

In model given by Eq. (1), function $\mathrm{f}$ is observed in a multiplicative signal-independent-noise $\mathbf{X}$ or, equivalently, in an additive signal-dependent-noise $\mathrm{f}(\mathbf{X} - 1)$.

[1] LISTIC, Université de Savoie - Polytech Annecy-chambéry, France, *Abdourrahmane.Atto@univ-savoie.fr*

[2] LISTIC, Université de Savoie - Polytech Annecy-chambéry, France, *Emmanuel.Trouve@univ-savoie.fr*

[3] LTCI, CNRS UMR 5141, Telecom ParisTech, 46 rue Barrault, 75013 Paris, France, *Jean-Marie.Nicolas@telecom-paristech.fr*

Given a transform $\mathcal{W}$ for analyzing $\mathbf{y}$, the issue addressed in this paper is analyzing multiplicative and additive frameworks for the representation of $\mathbf{y}$. We assume that the properties desired for $\mathcal{W}$ are both i) sparsity of representation of $\mathrm{f}$ and ii) simplifying the statistical properties of the noise involved in the model. In this respect, the transform $\mathcal{W}$ will be associated to wavelet operators.

In the following, $\mathcal{W}[\mathrm{f}\mathbf{X}]$ refer to

- the (standard) additive wavelet transform, with (linearity with respect to '+' operation):

$$\mathcal{W}\mathbf{y} = \mathcal{W}\mathrm{f} + \mathcal{W}\mathrm{f}(\mathbf{X} - 1), \qquad (\clubsuit)$$

- the multiplicative (or *geometric*) wavelet transform, with (multiplicative linearity where $\mathcal{W}$ distributes over '$\times$' operation):

$$\mathcal{W}\mathbf{y} = (\mathcal{W}\mathrm{f}) \times (\mathcal{W}\mathbf{X})\,. \qquad (\spadesuit)$$

The term geometric wavelet is used because approximations based on multiplicative operations are referred in the literature as geometric approximations: for instance, the mean value is known as *geometric mean* when it applies over '$\times$' operators.

Wavelets can be 'embedded' in a multiplicative algebra so that their decompositions (*geometric approximation* and *geometric differencing*) involve exactly the operations used in ($\spadesuit$). This embedding considers changing the algebra by using *binary internal multiplication* and *external power operation*. In this respect, the geometric approach involved in the paper contrasts significantly with 'curvature' based approaches (curvelets, bandlets, *etc*, see [8] [9], [10], [11] for instance). Note that the same approach can be used to define geometric curvelets, bandlets, *etc.*, on multiplicative algebras.

The paper is organized as follows: Section II provides statistical properties of additive wavelet based transforms on model ($\clubsuit$). The geometric wavelet transform is defined in Section III. Its statistical properties on model ($\spadesuit$) are discussed in the same section. Section IV concludes the work. From now on, we assume that $\mathbf{X} = (\mathbf{X}[\mathrm{k}])_{\mathrm{k}\in\mathbb{Z}}$ denotes a stationary sequence of strictly positive real random variables.

## II. Wavelet transform and multiplicative models

### A. Basics on wavelet based transforms

In the following, we are interested in multi-scale decomposition schemes involving paraunitary filters $(\mathbf{H_0}, \mathbf{H_1})$, where

$$\mathbf{H}_\epsilon(\omega) = \frac{1}{\sqrt{2}} \sum_{\ell \in \mathbb{Z}} \mathbf{h}_\epsilon[\ell] \mathbf{e}^{-i\ell\omega}, \quad \epsilon \in \{0,1\}, \tag{2}$$

and the paraunitarity of pair $(\mathbf{H_0}, \mathbf{H_1})$ is equivalent to saying that the matrix

$$M(\omega) = \begin{pmatrix} \mathbf{H}_0(\omega) & \mathbf{H}_1(\omega) \\ \mathbf{H}_0(\omega+\pi) & \mathbf{H}_1(\omega+\pi) \end{pmatrix} \tag{3}$$

is unitary for every $\omega$, see [12], among other references.

A one-level wavelet decomposition involves splitting [13] a given functional space $\mathbf{W}_{j,n} \subset L^2(\mathbb{R})$, defined as the closure of the space spanned $\{\tau_{2^j k} W_{j,n} : k \in \mathbb{Z}\}$ into direct sums of subspaces $(\mathbf{W}_{j+1,2n+\epsilon})_{\epsilon\in\{0,1\}}$, spanned respectively by $\{\tau_{2^{j+1}k} W_{j+1,2n+\epsilon} : k \in \mathbb{Z}\}_{\epsilon\in\{0,1\}}$, where $\tau_k f : t \longmapsto f(t-k)$. The splitting of $\mathbf{W}_{j,n}$ follows from decimated arithmetic convolution operations:

$$W_{j+1,2n+\epsilon}(t) = \sum_{\ell\in\mathbb{Z}} \mathbf{h}_\epsilon[\ell] W_{j,n}(t-2\ell). \tag{4}$$

for $\epsilon \in \{0,1\}$, where $\mathbf{h}_\epsilon$ denotes the impulse response of the *scaling filter* (when $\epsilon = 0$) or the wavelet filter (when $\epsilon = 1$).

The consequence of Eq. (4) is that a function $g$ having coefficients $c = (c[\ell])_{\ell\in\mathbb{Z}} \in \ell^2(\mathbb{Z})$ on $\{\tau_{2^j k} W_{j,n} : k \in \mathbb{Z}\}$:

$$g = \sum_{\ell\in\mathbb{Z}} c[\ell] \tau_{2^j \ell} W_{j,n} \in \mathbf{W}_{j,n}$$

can be expanded[1] [12] in terms of

$$g = \underbrace{\sum_{\ell\in\mathbb{Z}} c_0[\ell] \tau_{2^{j+1}\ell} W_{j+1,2n}}_{\in \mathbf{W}_{j+1,2n}} + \underbrace{\sum_{\ell\in\mathbb{Z}} c_1[\ell] \tau_{2^{j+1}\ell} W_{j+1,2n+1}}_{\in \mathbf{W}_{j+1,2n+1}}$$

where its coefficients $c_\epsilon = (c_\epsilon[\ell])_{\ell\in\mathbb{Z}}$ on $\{\tau_{2^{j+1}k} W_{j+1,2n+\epsilon} : k \in \mathbb{Z}\}_{\epsilon\in\{0,1\}}$, for $\epsilon \in \{0,1\}$, where

$$c_\epsilon[k] = \sum_{\ell\in\mathbb{Z}} \mathbf{h}_\epsilon[\ell] c[\ell - 2k]. \tag{5}$$

Starting the decomposition from a function $f \in \mathbf{W}_{0,0}$,

$$f = \sum_{\ell\in\mathbb{Z}} c[\ell] \tau_\ell W_{0,0},$$

the subband $W_{j,n}$ coefficients of $f$ follow from

$$c_{j,n}[k] = \sum_{\ell\in\mathbb{Z}} \mathbf{h}_{j,n}[\ell] c[\ell - 2^j k]. \tag{6}$$

where the Fourier transform $\mathbf{H}_{j,n}$ of $\mathbf{h}_{j,n}$ is (see [14, Eq. (26)]):

$$\mathbf{H}_{j,n}(\omega) = 2^{j/2} \left[ \prod_{\ell=1}^{j} \mathbf{H}_{\epsilon_\ell}(2^{\ell-1}\omega) \right]. \tag{7}$$

[1] Equalities hold in $L^2(\mathbb{R})$ sense in these expansions.

Eq. (6) can be used in practice for computing discrete wavelet transforms from sample observations (terminologies of 'discrete wavelet transform' when $n \in \{0,1\}$, 'discrete wavelet packet transform' when $n \in \{0,1,\ldots,2^j-1\}$, 'adapted discrete wavelet packets' for a suitable selection of $n$-indices). Some splitting schemes involving non-decimation (factor $2^j$ in Eq. (6)) are also available and yield to the concept of frames and the notion of stationary wavelet transforms [15]. The reader can refer to the abundant literature on wavelets for more details on wavelet transforms.

### B. Additive wavelet transform and multiplicative observation model - Sparsity checking

Sparsity plays a main role for simplifying image storage and processing. For piecewise smooth signals, sparsity follows from the differencing operated by wavelet functions and the corresponding differences are called details (scaling functions operate as approximation functions).

In the rest of the paper, we consider the application domain of Synthetic Aperture Radar (SAR) imaging.

In SAR imaging systems (characterized by multiplicative interactions between coherent waves and ground surface), the literature used to admit that the acquired SAR images are not very sparse in the wavelet domain . In this respect, adaptive lifting wavelets [16] or redundant wavelet frames [17] are more often used for analysis purpose in order to encompass this lacks of strong sparsity.

Figure 1 presents a polarimetric Synthetic Aperture Radar (SAR) image acquired by the DLR F-SAR sensor over the site of Kaufbeuren, Germany. The acquisition is performed by using coherent and polarized waves: Horizontal (H)/Vertical(V) for wave emission and Horizontal/Vertical for wave reception. Those polarimetric data are usually represented as a matrix of complex numbers composed by the 4 channels HH, HV, VH and VV and we have focused on the magnitudes of those complex data for image display. This display, see Figure 1, is a color composition where channels HH, HV and VV are associated with colors blue, green and red respectively. This image illustrates multiplicative scattering phenomenons in the different polarimetry channels.

Figure 2 provide standard (additive) detail wavelet coefficients of polarimetric data used to generate the image of Figure 1. The decomposition used is separable with respect to the different polarimetry channels and the Haar wavelet has been used for this decomposition.

In those detail coefficients (see Figure 2) issued from additive wavelets on a multiplicative observation model, we observed many structures of the scene under consideration. In particular, we observe even regular structures, which, obviously might not be present in detail wavelet

coefficients: regular structures are the domain of the scaling function and details must not contain rich structural information in case of strong sparsity.

Approximation coefficients are not provided: they look very similar for additive and multiplicative wavelet implementations, the few differences of perception are linked to edges and contours: such transition involve a wide range of real numbers (transition model) and in this case, the geometric approximation is known to have a higher compacity property than the arithmetic approximation (a small range in the geometric mean corresponds to a wider range in the arithmetic mean).

Note that sparsity is a property applying on $f$. However, in a noisy environment, the useful sparsity is strongly linked to the noise properties since noise affects the non-zero coefficients and thus, affects the quality of the approximation that can be obtained by considering those non-zero coefficients. In this respect, the following addresses the properties of wavelet functions of the noise involved in (♣).

### *C. Stochasticity and the additive wavelet decomposition*

In model (♣), the additive noise contribution is associated with a random sequence having the form

$$\mathbf{Y}[k] = f[k](\mathbf{X}[k] - 1). \tag{8}$$

Since we have assumed that $(\mathbf{X}[k])_{k\in\mathbb{Z}}$ are stationary with $\mathbb{E}\mathbf{X}[k] = \mu_0$ and autocorrelation function $R_{\mathbf{X}}[k,\ell] = \mathbb{E}\left[\mathbf{X}[k]\mathbf{X}[\ell]\right] \triangleq R_{\mathbf{X}}[k-\ell]$, then:

- The mean of $\mathbf{Y}[k]$ is

$$\mathbb{E}\mathbf{Y}[k] = f[k](\mu_0 - 1). \tag{9}$$

- The autocorrelation function of $\mathbf{Y}$, $R_{\mathbf{Y}}[k,\ell] = \mathbb{E}\left[\mathbf{Y}[k]\mathbf{Y}[\ell]\right]$ satisfies, by taking into account Eq. (8):

$$R_{\mathbf{Y}}[k,\ell] = f[k]f[\ell]\left(R_{\mathbf{X}}[k-\ell] - 1\right). \tag{10}$$

*Remark 1:* Eqs. (9) and (10) above highlights that the additive signal-dependent noise $\mathbf{Y}$ is non-stationary in general, excepted some few cases, for instance when $f$ is constant.

Let us now analyze the wavelet coefficients of $\mathbf{Y}$. Denote by $\mathbf{C}^+_{j,n}$ the coefficients of $\mathbf{Y}$ on subband $\mathbf{W}_{j,n}$. We have

$$C^+_{j,n}[k] = \sum_{\ell\in\mathbb{Z}} \mathbf{h}_{j,n}[\ell] f[\ell - 2^j k](\mathbf{X}[\ell - 2^j k] - 1). \tag{11}$$

It follows that

$$\mathbb{E}C^+_{j,n}[k] = (\mu_0 - 1)\sum_{\ell\in\mathbb{Z}} \mathbf{h}_{j,n}[\ell] f[\ell - 2^j k] \tag{12}$$

and the autocorrelation function $R^+_{j,n}[k,\ell] = \mathbb{E}C^+_{j,n}[k]C^+_{j,n}[\ell]$ of $C^+_{j,n}$ is

$$R^+_{j,n}[k,\ell] = \sum_{p\in\mathbb{Z}}\sum_{q\in\mathbb{Z}} \mathbf{h}_{j,n}[p]h_{j,n}[q]\times f[p - 2^j k]f[q - 2^j \ell]\times \left(R_{\mathbf{X}}[p - q - 2^j(k-\ell)] - 1\right) \tag{13}$$

From Eqs. (12) and (13), we derive that $C^+_{j,n}$ non-stationary in general, for instance when $\mu_0 \neq 1$. When $\mu_0 = 1$, non-stationarity is due to the presence of the term $f[p - 2^j k]f[q - 2^j \ell]$ in Eq. (13).

*Remark 2 (Non-stationarity of $C^+_{j,n}$ for exponential type function $f$):* Assume that $\mu_0 = 1$ and function $f$ satisfies $f[k]f[\ell] = f[k+\ell]$ (exponential type functions), where $f$ does not reduce to the constant 1. In this case, we derive

$$R^+_{j,n}[k,\ell] = \frac{f[-2^j(k+\ell)]}{2\pi} \times \int_{-\pi}^{\pi} \gamma_{\mathbf{X}^0}(\omega)\left|G_{j,n}(\omega)\right|^2 e^{i2^j(k-\ell)\omega}\, d\omega \tag{14}$$

where $G_{j,n} = F * \mathbf{H}_{j,n}$ and $F$ is the Fourier transform of $f$. The non-stationarity of $C^+_{j,n}$ is then due to the term $f[-2^j(k+\ell)]$ in Eq. (14) above.

More generally, even when assuming that $\mu_0 = 1$, it is easy to check that most standard functions $f$ lead to non-stationarity of $C^+_{j,n}$. In particular, linear functions of type $f[k] = f_0 \times k$ (for certain $k$ in a finite set) have a term in $k\ell$ which cannot be simplified in $R^+_{j,n}[k,\ell]$. High order polynomial functions have bivariate monomial terms involving $k^\lambda \ell^\eta$ in $R^+_{j,n}[k,\ell]$. Functions of type $\sin, \cos$ satisfy $f[k]f[\ell] = g_1[k+\ell] + g_2[k-\ell]$ and in this case, the contribution of $g_1$ implies non-stationarity as in the exponential case given above, *etc.* For a practical viewpoint, this non-stationary is simply emphasized by Figure 2: in the areas where $f$ is not constant, many f-structures (buildings)/f-texture (forest) are present in detail wavelet coefficients.

An appealing case of stationarity sequence $C^+_{j,n}$ corresponds to a constant function $f$ associated with a random sequence $\mathbf{X}$ with unit mean:

*Remark 3 (Stationarity):* When $\mu_0 = 1$ and $f$ is a constant function: $f[k] = f_0$, then $\mathbb{E}C^+_{j,n}[k] = 0$ and furthermore, we derive $R^+_{j,n}[k,\ell] = R^+_{j,n}[k-\ell] = R^+_{j,n}[m]$ with:

$$R^+_{j,n}[m] = \frac{f_0^2}{2\pi}\int_{-\pi}^{\pi} \gamma_{\mathbf{X}^0}(\omega)\left|\mathbf{H}_{j,n}(\omega)\right|^2 e^{i2^j m\omega}\, d\omega \tag{15}$$

where $\gamma_{\mathbf{X}^0}$ denotes the spectrum of the random sequence $\mathbf{X}^0 = \mathbf{X} - 1$.

$$\gamma_{\mathbf{X}^0}(\omega) = \sum_{m\in\mathbb{Z}} \left(R_{\mathbf{X}}[m] - 1\right) e^{-im\omega}.$$

This case of a constant function f observed in a multiplicative noise represents homogeneous area observation in practical SAR applications. This case is the sole favorable scenario for standard additive wavelets when the challenge is simplifying the multiplicative model $f\mathbf{X}$.

Due to the non-stationarity of $C^{+}_{j,n}$ in general (excepted few cases such as that of Remark 3), modeling or estimating additive wavelet coefficients of a multiplicative model is not an easy task. The following highlights that multiplicative implementations of wavelets is more convenient for the statistical analysis of model $f\mathbf{X}$.

## III. Embedding wavelets in a multiplicative algebra

### A. Geometric convolution

The binary operation considered in the following is the multiplication ($\times$ symbol) over positive real numbers $\mathbb{R}^+$ ("0" has no sign and is not considered as a positive number).

Consider a data sequence $\mathbf{x} = (\mathbf{x}[\ell])_{\ell\in\mathbb{Z}}$, with $\mathbf{x}[\ell] \in \mathbb{R}^+$ for every $\ell \in \mathbb{Z}$. Since this sequence represents a multiplicative phenomena, then

- "zero" or "nothing" or "no change" corresponds to the identity element "1"
- a "small" value is a value close to 1 ($10^{-3}$ and $10^{3}$ have the same significance in terms of *absolute proportion*,
- a missing value must be replaced by 1,
- shrinkage designate forcing to 1, the coefficients that are close to 1.

The multiplicative algebra implies defining the support of the sequence $\mathbf{x}$ as the sub-sequence composed with elements that are different from 1. We will thus use the standard terminologies of finite/infinite supports with respect to the above remark. When such a sequence $\mathbf{x}$ is infinite, we will assume that $\log(\mathbf{x}) = ((\log \mathbf{x}[k])_{k\in\mathbb{Z}}) \in \ell^2(\mathbb{Z})$.

When considering a scalar sequence (impulse response of a filter for instance) $\mathbf{h} = (\mathbf{h}[\ell])_{\ell\in\mathbb{Z}}$ where $\mathbf{h}[\ell] \in \mathbb{R}$ for every $\ell \in \mathbb{Z}$, then we will keep the standard terminology related to support definition from non-zero elements (non-null real numbers).

The geometric convolution defined below is based on this binary operation (notation $x \times y \triangleq xy$ for $x, y \in \mathbb{R}^+$) and real scalar power operations (notation $a \wedge x \triangleq x^a$ for $x \in \mathbb{R}^+$ and $a \in \mathbb{R}$).

*Definition 1 (Geometric convolution):* Let $\mathbf{h} = (\mathbf{h}[\ell])_{\ell\in\mathbb{Z}}$ denotes the impulse response of a digital filter. We define the geometric convolution of $\mathbf{x}$ and $\mathbf{h}$ on the vectorial space $(\mathbb{R}^+, \times, \wedge)$ as:

$$\mathbf{y}[k] = \mathbf{x} \circledast \mathbf{h}[k] \triangleq \prod_{\ell\in\mathbb{Z}} (\mathbf{x}[\ell])^{\mathbf{h}[k-\ell]} = \prod_{\ell\in\mathbb{Z}} (\mathbf{x}[k-\ell])^{\mathbf{h}[\ell]} \triangleq \mathbf{h} \circledast \mathbf{x}[k], \quad (16)$$

One can remark that, in contrast with the standard convolution operation on the sequences of the field $(\mathbb{R}, +, \times)$, sequence $\mathbf{h}$ plays a non-commutative scalar role with respect to $\mathbf{x}$ since the external operation 'power' used in Eq. (16) is not commutative. This justifies the second $\triangleq$ in Eq. (16): the equality $\mathbf{x} \circledast \mathbf{h} = \mathbf{h} \circledast \mathbf{x}$ applies index-wise on the geometric convolution, given that the scalar sequence $\mathbf{h}$ operates to the power of elements of $\mathbf{x}$, by definition.

If $\mathbf{h} \in \ell^2(\mathbb{Z})$, then $\mathbf{x} \circledast \mathbf{h}[k]$ exists and is finite for almost ever $k$ since we have assumed that $\log(\mathbf{x}) \in \ell^2(\mathbb{Z})$.

Depending on the filter $\mathbf{h}$ used, Eq. (16) makes possible the computation of geometric approximations and differences of the input data $\mathbf{x}$. The standard geometric approximation (called *geometric mean*) of a finite sequence $\{x_1, x_2, \ldots, x_N\}$ is given by:

$$y = \sqrt[N]{x_1 x_2 \cdots x_N} = \prod_{\ell=1}^{N} x_\ell^{1/N}. \quad (17)$$

The geometric mean given by Eq. (17) above is associated with an N-length Haar-like scaling filter

$$\mathbf{h_0}[k] = \nu \text{ for } k = 1, 2, \ldots, N. \quad (18)$$

Filter $\mathbf{h_0}$ (*low pass filter*) performs geometric approximations and can be associated with a Haar-like wavelet filter

$$\mathbf{h_1}[k] = (-1)^{k-1}\nu \text{ for every } k = 1, 2, \ldots, N. \quad (19)$$

which performs geometric differencing (*high pass* or details), where constant $\nu > 0$ is fixed so as to impose paraunitarity for the corresponding pair of filters ($\nu = \sqrt{2}/2$ for standard Haar filters when $N = 2$).

### B. Geometric wavelet decomposition

In the following, we consider the same paraunitary *wavelet filters* $(\mathbf{h}_0, \mathbf{h}_1) \in \ell^2(\mathbb{Z}) \times \ell^2(\mathbb{Z})$ as in Section II. Let

$$\overline{\mathbf{h}[k]} = \mathbf{h}[-k].$$

Define the wavelet decomposition of $\mathbf{x}$ with respect to the geometric convolution (*geometric wavelet decomposition*) by:

$$\mathbf{c}_{1,0}[k] = \mathbf{x} \circledast \overline{\mathbf{h}_0}[2k], \quad (20)$$

$$\mathbf{c}_{1,1}[k] = \mathbf{x} \circledast \overline{\mathbf{h}_1}[2k], \quad (21)$$

and, recursively, for $\epsilon \in \{0, 1\}$ (wavelet packet splitting formalism described in [13]):

$$\mathbf{c}_{j+1,2n+\epsilon}[k] = \mathbf{c}_{j,n} \circledast \overline{\mathbf{h}_\epsilon}[2k]. \quad (22)$$

In the decomposition given by Eq. (22) above, sequence $\mathbf{c}_{j+1,2n+\epsilon}$ represents

- geometric approximations of $\mathbf{c}_{j,n}$ when $\epsilon = 0$
- geometric differences (details) of $\mathbf{c}_{j,n}$ when $\epsilon = 1$.

The level $j = 0$ coefficients represent the input sequence $\mathbf{x}$. The above wavelet packet splitting is associated to a wavelet decomposition when the splitting concerns only $(\mathbf{c}_{j,0})_{j\geqslant 1}$

***Proposition** 1 (Geometric wavelet reconstruction):* We have:

$$\mathbf{c}_{j,n}[k] = (\check{\mathbf{c}}_{j+1,2n} \circledast \mathbf{h}_0[k]) \times (\check{\mathbf{c}}_{j+1,2n+1} \circledast \mathbf{h}_1[k])\,. \quad (23)$$

where

$$\check{\mathbf{u}}[2k+\epsilon] = \begin{cases} \mathbf{u}[k] & \text{if} \quad \epsilon = 0, \\ 1 & \text{if} \quad \epsilon = 1. \end{cases} \quad (24)$$

*Proof:* The proof is a direct consequence of the expansion of the right hand side of Eq. (23), by taking into account Eq. (22) and the paraunitary condition of Eq. (3), the latter imposing $\sum_{\ell\in\mathbb{Z}} \mathbf{h}_\epsilon[\ell]\overline{\mathbf{h}_\epsilon}[\ell - 2k] = \delta[k]$. ■

Proposition 1 represents the reconstruction of the level-$j$-wavelet-coefficients from the coefficients located at level $j + 1$. As in the standard additive formulation given in Section II (see Eq. (5)), different wavelet decomposition schemes (orthogonal wavelets, stationary wavelets, adapted wavelet packets, *etc.*) and perfect reconstructions can be obtained from Eqs. (22) and (23) respectively. For implementing the geometric transforms from the standard ones, it suffices to

- replace the standard convolution by the geometric convolution given in Definition 1 and
- notice that decimation corresponds to replacing one coefficients over two by the number 1.

In the following, we will address the statistical properties of the coefficients issued from Eq. (22).

### *C. Multiplicative wavelet transform and multiplicative observation model - Sparsity checking*

Section II-B has emphasized the lack of sparsity of the additive wavelet details when dealing with a multiplicative observation model (see Figure 2 for instance). In order to seek sparse detail representations for this model, changing wavelet functions by considering another class of basis functions is not the issue to address: we just need to apply a convolution operation adapted to our sampling process. Indeed, since a given natural scene (such as that of Figure 1) can be coarsely described as a piecewise smooth function, then wavelets are expected to capture the intrinsic redundancy of such a scene in a sparse way, independently of the intrinsic properties of the acquisition device.

For the SAR images, this operation is described by a multiplicative type interaction between signal and speckle noise. In this respect, wavelet based decompositions should also be multiplicative for sparsity to holds true in wavelet detail domain.

Figure 3 provide geometric (multiplicative) detail wavelet coefficients of polarimetric data used to generate the image of Figure 1. When analyzing these detail coefficients, we observe only a very few structures of input signal. Multiplicative wavelet details are thus more convenient for sparse based analysis than additive wavelet coefficients for this observation model. Note that for the multiplicative model (♠), sparsity denotes a large number of 'ones' and detail wavelet images of Figure 3 have been displayed in a logarithmic scale so as to make comparison with Figure 2 possible.

### *D. Stochasticity and the geometric wavelet decomposition*

In model (♠), noise contribution is multiplicative and associated with a unit-mean stationary random sequence $\mathbf{X} = (\mathbf{X}[k])_{k\in\mathbb{Z}}$. Note that the geometric wavelet decomposition of Eq. (22), say $\mathcal{W}^\times$, distributes over the product $f\mathbf{X}$: $\mathcal{W}^\times[f\mathbf{X}] = (\mathcal{W}^\times f)\,(\mathcal{W}^\times \mathbf{X})$. In this respect, the focus of this Section are the statistical properties of $\mathcal{W}^\times\mathbf{X}$. The subband $\mathbf{W}_{j,n}$ geometric wavelet coefficients of the decomposition of $\mathbf{X}$ will be denoted $(\mathbf{C}^\times_{j,n})_{j,n}$ (we assume that this stochastic sequence is well defined in the following).

Note that if $\mathbf{C}_{j+1,2n+\epsilon}[k] = \mathbf{C}_{j,n} \circledast \overline{\mathbf{h}_\epsilon}[2k]$ where $\mathbf{C}_{j,n}$ is a stationary sequence, then $\mathbf{C}_{j+1,2n+\epsilon}$ is also stationary. Since $\mathbf{C}_{0,0} = \mathbf{X}$ is assumed stationary, we derive that all geometric wavelet sequences $\mathbf{C}_{j,n}$ are stationary for $j \geqslant 0$ and $n \in \{0, 1, \ldots, 2^j - 1\}$.

Let $\mathbf{Y} = \log \mathbf{X}$. We assume hereafter that $\mathbf{Y}$ is a second-order random process, continuous in quadratic mean. Let $\mathbf{D}_{j,n} = \log \mathbf{C}^\times_{j,n}$. Note that $\mathbf{Y}$ and $\mathbf{D}_{j,n}$ are stationary sequences. Assume that $\mathbb{E}\mathbf{Y}[k] = 0$ for every $k \in \mathbb{Z}$. Then $\mathbb{E}\mathbf{D}_{j,n}[k] = 0$ for every $k \in \mathbb{Z}$.

Let $R_{\mathbf{Y}}[m] = R_{\mathbf{Y}}[k-\ell] = \mathbb{E}\,[\mathbf{Y}[k]\mathbf{Y}[\ell]]$ be the autocorrelation function of $\mathbf{Y}$, where the first equality above holds true for any pair $(k, \ell) \in \mathbb{Z} \times \mathbb{Z}$ such that $m = \pm|k - \ell|$. Proposition 2 below derives the autocorrelation function $R_{\mathbf{D}_{j,n}}$ of the log-scaled geometric wavelet coefficient $\mathbf{D}_{j,n}$. We assume that $\sum_{q\in\mathbb{Z}} \mathbf{h}_\epsilon[p - 2k]\mathbf{h}_\epsilon[q - 2\ell]R_{\mathbf{D}_{j,n}}[p, q]$ exists for every $j \geqslant 0$ and $n \in \{0, 1, \ldots, 2^j - 1\}$.

***Proposition** 2 (Autocorrelation Function of $\mathbf{D}_{j,n}$):* Assume that $R_{\mathbf{Y}}$ has a spectrum (power spectral density)

$$\gamma_{\mathbf{Y}}(\omega) = \sum_{m\in\mathbb{Z}} R_{\mathbf{Y}}[m]e^{-im\omega}$$

and that $\gamma_{\mathbf{Y}}$ is bounded. Denote by $\gamma_{\mathbf{D}_{j,n}}$, the spectrum

of $\mathbf{D}_{j,n}$:

$$\gamma_{\mathbf{D}_{j,n}}(\omega) = \sum_{m\in\mathbb{Z}} R_{\mathbf{D}_{j,n}}[m]e^{-im\omega} \quad (25)$$

We have, for $j \geqslant 0$, $n \in \{0,1,\ldots,2^{j-1}\}$ and $\epsilon \in \{0,1\}$:

$$R_{\mathbf{D}_{j+1,2n+\epsilon}}[m] = \frac{1}{2\pi}\int_{-\pi}^{\pi} \left|\widehat{\mathbf{H}_\epsilon}(\omega)\right|^2 \gamma_{\mathbf{D}_{j,n}}(\omega)e^{2im\omega}\,d\omega \quad (26)$$

where $\gamma_{\mathbf{D}_{0,0}} = \gamma_{\mathbf{Y}}$.

*Proof:* By considering the log of $\mathbf{C}^{\times}_{j+1,2n+\epsilon}$ denoted by $\mathbf{D}_{j+1,2n+\epsilon}$, we are concerned by an additive combinations of $\mathbf{D}_{j,n} = \log \mathbf{C}^{\times}_{j,n}$.

The autocorrelation functions $R_{\mathbf{D}_{j+1,2n+\epsilon}}[k,\ell] = \mathbb{E}\mathbf{D}^{+}_{j+1,2n+\epsilon}[k]\mathbf{D}^{+}_{j+1,2n+\epsilon}[\ell]$ and $R_{\mathbf{D}_{j,n}}[k,\ell] = \mathbb{E}\mathbf{D}^{+}_{j,n}[k]\mathbf{D}^{+}_{j,n}[\ell]$ of $C^{+}_{j,n}$ satisfy the relation:

$$R_{\mathbf{D}_{j+1,2n+\epsilon}}[k,\ell] = \sum_{p\in\mathbb{Z}}\sum_{q\in\mathbb{Z}} \mathbf{h}_\epsilon[p-2k]\mathbf{h}_\epsilon[q-2\ell]\times R_{\mathbf{D}_{j,n}}[p,q] \quad (27)$$

Since $\mathbf{D}_{j,n}$ is stationary: $R_{\mathbf{D}_{j,n}}[p,q] \triangleq R_{\mathbf{D}_{j,n}}[p-q]$, then Eq. (27) can be rewritten in the form

$$R_{\mathbf{D}_{j+1,2n+\epsilon}}[k,\ell] = \sum_{p\in\mathbb{Z}} R_{\mathbf{D}_{j,n}}[p]\times \sum_{q\in\mathbb{Z}} \mathbf{h}_\epsilon[p+q-2k]\mathbf{h}_\epsilon[q-2\ell]. \quad (28)$$

By taking into account that (Parseval's theorem):

$$\sum_{q\in\mathbb{Z}} \mathbf{h}_\epsilon[p+q-2k]\mathbf{h}_\epsilon[q-2\ell] = \sum_{q\in\mathbb{Z}} \tau_{2k-2\ell-p}\mathbf{h}_\epsilon[q]\mathbf{h}_\epsilon[q] = \frac{1}{2\pi}\int_{-\pi}^{\pi} \left|\widehat{H_\epsilon}(\omega)\right|^2 e^{i(2k-2\ell-p)\omega}\,d\omega, \quad (29)$$

we obtain from Eq. (28):

$$R_{\mathbf{D}_{j+1,2n+\epsilon}}[k,\ell] = \frac{1}{2\pi}\int_{-\pi}^{\pi} e^{i(2k-2\ell)\omega}\left|\widehat{\mathbf{H}_\epsilon}(\omega)\right|^2 \times \left(\sum_{p\in\mathbb{Z}} R_{\mathbf{D}_{j,n}}[p]e^{-ip\omega}\right) \quad (30)$$

The proof follows from Eq. (25) and Eq. (30), by identifying the Fourier expansion of $\gamma_{\mathbf{D}_{j,n}}$ in Eq. (30) and by noting that $R_{\mathbf{D}_{j+1,2n+\epsilon}}[p,q] \triangleq R_{\mathbf{D}_{j+1,2n+\epsilon}}[p-q] = R_{\mathbf{D}_{j+1,2n+\epsilon}}[m]$ where $m = k-\ell$. ■

By taking into account that sequence $\mathbf{D}_{j,n}$ issues from a filter bank $(H_{\epsilon_\ell})_{\ell=1,2,\ldots,j}$ (low-pass when $\epsilon_\ell = 0$ and high-pass when $\epsilon_\ell = 1$) having the equivalent representation given by Eq. (7), we derive recursively from Eq. (26):

$$R_{\mathbf{D}_{j,n}}[m] = \frac{1}{2\pi}\int_{-\pi}^{\pi} |\mathbf{H}_{j,n}(\omega)|^2 \gamma_{\mathbf{Y}}(\omega)e^{2^j im\omega}\,d\omega \quad (31)$$

Eq. (31) governs the behavior of the autocorrelation of $\mathbf{D}_{j,n}$. From this equation, decorrelating geometric wavelet coefficients involves selecting wavelet filters such that

$$\frac{1}{2\pi}\int_{-\pi}^{\pi} |\mathbf{H}_{j,n}(\omega)|^2 \gamma_{\mathbf{Y}}(\omega)\cos 2^j m\omega\,d\omega \quad (32)$$

behaves approximately as $\delta[m]$. This is strongly linked to the shape of $\gamma_{\mathbf{Y}}$ and can be achieved by

(i) choosing a sequence of wavelet filters such that function $|\mathbf{H}_{j,n}(\omega)|^2\gamma_{\mathbf{Y}}(\omega)$ can be seen as approximately constant or

(ii) seeking for asymptotic decorrelation with $j$, when it applies.

Item (i) is parametric in the sense that it relates to adapted wavelet selection for decorrelating $\mathbf{Y}$. Item (ii) (non-parametric) exploits properties of recursive convolutions. For instance, if we consider the Haar wavelet filters (used below for experimental results), we can derive :

***Proposition 3** (Haar equivalent wavelet filter sequence $\mathbf{H}^{Haar}_{j,n}$):* A sequence $(\mathbf{h}_{\epsilon_\ell})_{\ell=1,2,\ldots,j}$ has equivalent filter:

$$\left|\mathbf{H}^{\mathrm{Haar}}_{j,n}(\omega)\right|^2 = 2^j\prod_{\ell=1}^{j}\cos^2\left(2^{\ell-2}\omega + \epsilon_\ell\frac{\pi}{2}\right). \quad (33)$$

*Proof:* Let $\epsilon \in \{0,1\}$. The Haar scaling filter $\mathbf{H}^{\mathrm{Haar}}_0$ and wavelet filter $\mathbf{H}^{\mathrm{Haar}}_1$ satisfies

$$\mathbf{H}^{\mathrm{Haar}}_\epsilon(\omega) = \frac{1}{2}\left(1+(1-2\epsilon)e^{-i\omega}\right) \quad (34)$$

By taking into account Eqs. (7) and (34), we have

$$\mathbf{H}^{\mathrm{Haar}}_{j,n}(\omega) = 2^{-j/2}\prod_{\ell=1}^{j}\left(1+(1-2\epsilon_\ell)e^{-i\omega}\right). \quad (35)$$

Thus,

$$\left|\mathbf{H}^{\mathrm{Haar}}_{j,n}(\omega)\right|^2 = \prod_{\ell=1}^{j}\left(1+(1-2\epsilon_\ell)\cos(2^{\ell-1}\omega)\right). \quad (36)$$

The proof follows by noting that $(1-2\epsilon_\ell)\cos(2^{\ell-1}\omega) = \cos(2^{\ell-1}\omega+\epsilon_\ell\pi)$ and after some straightforward simplifications by using trigonometry double angle properties. ■

In the usual wavelet splitting scheme, only approximation coefficients are decomposed again (the shift parameter $n \in \{0,1\}$). This implies filtering sequences with the form

$$\left(\underbrace{\mathbf{h}_0,\mathbf{h}_0,\ldots,\mathbf{h}_0}_{j\text{ times}},\mathbf{h}_{\epsilon_{j+1}}\right)_{\epsilon_{j+1}\in\{0,1\}}$$

at decomposition level $j+1$. Consider a $j$-length approximation sequence $\left(\mathbf{h}^{\mathrm{Haar}}_0\right)_{\ell=1,2,\ldots,j}$ of Haar type. Then from

Eq. (33), the equivalent filter of this sequence can be rewritten in the form:

$$\left|\mathbf{H}_{j,0}^{\text{Haar}}(\omega)\right|^2 = 2^j \left(\frac{\text{sinc}(2^{j-1}\omega)}{\text{sinc}(2^{-1}\omega)}\right)^2 \quad (37)$$

where sinc denotes the *cardinal sine* function, $\text{sinc}\omega = \sin\omega/\omega$. The autocorrelation $R_{\mathbf{D}_{j,0}}^{\text{Haar}}$ of the corresponding geometric wavelet coefficients is then:

$$R_{\mathbf{D}_{j,0}}^{\text{Haar}}[m] = \frac{2^j}{\pi}\int_0^{\pi}\left(\frac{\text{sinc}(2^{j-1}\omega)}{\text{sinc}(2^{-1}\omega)}\right)^2 \gamma_{\mathbf{Y}}(\omega)\cos 2^j m\omega\, d\omega \quad (38)$$

***Proposition** 4 (Limit Autocorrelation Function):*

$$\lim_{j\to+\infty} R_{\mathbf{D}_{j,0}}^{\text{Haar}}[m] = \gamma_{\mathbf{Y}}(0)\delta[m] \quad (39)$$

*Proof:*

From a change of variable in Eq. (38), we obtain

$$R_{\mathbf{D}_{j,0}}^{\text{Haar}}[m] = \frac{1}{\pi}\int_0^{2^j\pi}\left(\frac{\text{sinc}(\omega/2)}{\text{sinc}(\omega/2^{j+1})}\right)^2 \gamma_{\mathbf{Y}}(\frac{\omega}{2^j})\cos m\omega\, d\omega.$$

First, we observe that:

$$\left|R_{\mathbf{D}_{j,0}}^{\text{Haar}}[m]\right| \leqslant \|\gamma_{\mathbf{Y}}\|_\infty \times \left(\frac{1}{\pi}\int_0^{2^j\pi}\left(\frac{\text{sinc}(\omega/2)}{\text{sinc}(\omega/2^{j+1})}\right)^2 d\omega\right).$$

and, furthermore, we have

$$\frac{1}{\pi}\int_0^{+\infty}\left(\frac{\text{sinc}(\omega/2)}{\text{sinc}(\omega/2^{j+1})}\right)^2 d\omega = 1.$$

In this respect, we derive

$$\left|R_{\mathbf{D}_{j,0}}^{\text{Haar}}[m]\right| \leqslant \|\gamma_{\mathbf{Y}}\|_\infty$$

so that, from the Lebesgue dominated convergence theorem,

$$\lim_{j\to+\infty} R_{\mathbf{D}_{j,0}}^{\text{Haar}}[m] = \gamma_{\mathbf{Y}}(0)\frac{1}{\pi}\int_0^{+\infty}(\text{sinc}(\omega/2))^2\cos m\omega\, d\omega$$

Proposition 4 then follows by noting that

$$\int_0^{+\infty}(\text{sinc}(\omega/2))^2\cos m\omega\, d\omega = \pi\delta[m]$$

■

Proposition 4 highlights an asymptotic decorrelation property with j. This property can be extended by considering different wavelets and different wavelet packet splitting schemes, as done in [14] for the standard arithmetic wavelet transforms (we restrict to the Haar wavelets in a wavelet decomposition scheme, framework of the experimental results provided in the following section). From the stationarity and decorrelation properties shown in this section, it follows that Model (♣) is suitable for statistical analysis of observation f$\mathbf{X}$ since $\mathbf{X}$-wavelet coefficients define a stationary sequence $\mathbf{C}_{j,n}^{\times}$ (confirmation of the stationarity perception in Figure 3) and the form of the autocorrelation of this sequence can be specified for decorrelation purpose through a selection of adapted filter $\mathbf{H}_{j,n}$ in Eq. (31).

## IV. Conclusion

This paper has addressed the derivation of a geometric wavelet transform from inference between additive and multiplicative algebras. Sparsity and stochasticity properties of additive (arithmetic) and multiplicative (geometric) wavelet transforms have been discussed on a multiplicative observation model.

In the multiplicative noise model, the paper has shown that:

- concerning sparsity, additive detail wavelet coefficients are impacted by the presence of signal (large amount of signal contribution in detail coefficients), whereas few signal contributions occur in multiplicative detail coefficients.
- concerning stochasticity, geometric wavelets inherits stationary property of the input noise whereas additive stationary noise becomes non-stationary in the additive wavelet domain, due to the impact of noise-free signal in detail coefficients.

The paper concludes by noting that the selection of a suitable framework for analyzing signals/images should be acquisition-dependent. In particular, when the acquisition system yields a multiplicative interaction model involving a non-constant signal, then geometric representation frameworks such as that presented in this paper are expected to be more relevant than additive frameworks. This has been emphasized on SAR images corrupted by multiplicative speckle noise.

## References


[1] H. Xie, L. E. Pierce, and F. T. Ulaby, "Statistical properties of logarithmically tranformed speckle," *IEEE Transactions on Geoscience and Remote Sensing*, vol. 40, no. 3, pp. 721 – 727, Mar. 2002.

[2] R. Garcia, T. Nicosevici, and X. Cufi, "On the way to solve lighting problems in underwater imaging," in *OCEANS '02 MTS/IEEE*, vol. 2, 2002, pp. 1018–1024 vol.2.

[3] O. Michailovich and A. Tannenbaum, "Despeckling of medical ultrasound images," *Ultrasonics, Ferroelectrics and Frequency Control, IEEE Transactions on*, vol. 53, no. 1, pp. 64–78, 2006.

[4] L. Florack and H. Assen, "Multiplicative calculus in biomedical image analysis," *Journal of Mathematical Imaging and Vision*, vol. 42, no. 1, pp. 64–75, 2012. [Online]. Available: http://dx.doi.org/10.1007/s10851-011-0275-1

[5] P. Gould and F. Vahid-Araghi, "Time series with multiple seasonal patterns," in *Forecasting with Exponential Smoothing*, ser. Springer Series in Statistics. Springer Berlin Heidelberg, 2008, pp. 229–254. [Online]. Available: http://dx.doi.org/10.1007/978-3-540-71918-2_14

[6] M. Verbeek, *A Guide to Modern Econometrics, 4th Edition.* John Wiley & Sons, February 2012.

[7] J. M. Box-Steffensmeier and C. J. W. Zorn, "Duration models and proportional hazards in political science." Springer Berlin Heidelberg, 2001, vol. 45, no. 4, pp. 972–988.

[8] E. J. Candès and D. L. Donoho, "Curvelets - a surprisingly effective nonadaptive representation for objects with edges," *Curves and Surfaces, L. L. Schumaker et al. (eds), Vanderbilt University Press, Nashville, TN*, 2000.

Fig. 1. Polarimetric FSAR X-band image with size 5000 × 5000 over Kaufbeuren site, Germany. The sensor used for this acquisition operates in the spectral X-band, has altitude 3045 meter and offer a pixel spacing of 15 centimeter in range and 17 centimeter in azimuth.


[9] ——, "New tight frames of curvelets and optimal representations of objects with piecewise $C^2$ singularities," *Communications on Pure and Applied Mathematics, Wiley Periodicals, Inc., A Wiley Company*, vol. 57, no. 2, pp. 219 – 266, 2004.

[10] E. Candès, L. Demanet, D. Donoho, and L. Ying, "Fast discrete curvelet transforms," *Multiscale Modeling and Simulation*, vol. 5, no. 3, pp. 861 – 899, 2006.

[11] G. Peyré, C. Dossal, E. L. Pennec, and S. Mallat, "Geometric estimation with orthogonal bandlet bases," *In Proceedings of SPIE Wavelet XII*, 2007.

[12] S. Mallat, *A wavelet tour of signal processing, second edition.* Academic Press, 1999.

[13] I. Daubechies, *Ten lectures on wavelets.* SIAM, Philadelphie, PA, 1992.

[14] A. M. Atto and Y. Berthoumieu, "Wavelet packets of nonstationary random processes: Contributing factors for stationarity and decorrelation," *IEEE Transactions on Information Theory*, vol. 58, no. 1, Jan. 2012. [Online]. Available: http://dx.doi.org/10.1109/TIT.2011.2167496

[15] R. R. Coifman and D. L. Donoho, *Translation invariant denoising.* Lecture Notes in Statistics, 1995, no. 103, pp. 125 – 150.

[16] X. Hou, J. Yang, G. Jiang, and X. Qian, "Complex sar image compression based on directional lifting wavelet transform with high clustering capability," *Geoscience and Remote Sensing, IEEE Transactions on*, vol. 51, no. 1, pp. 527–538, 2013.

[17] J. Ranjani and S. Thiruvengadam, "Dual-tree complex wavelet transform based sar despeckling using interscale dependence," *Geoscience and Remote Sensing, IEEE Transactions on*, vol. 48, no. 6, pp. 2723–2731, 2010.

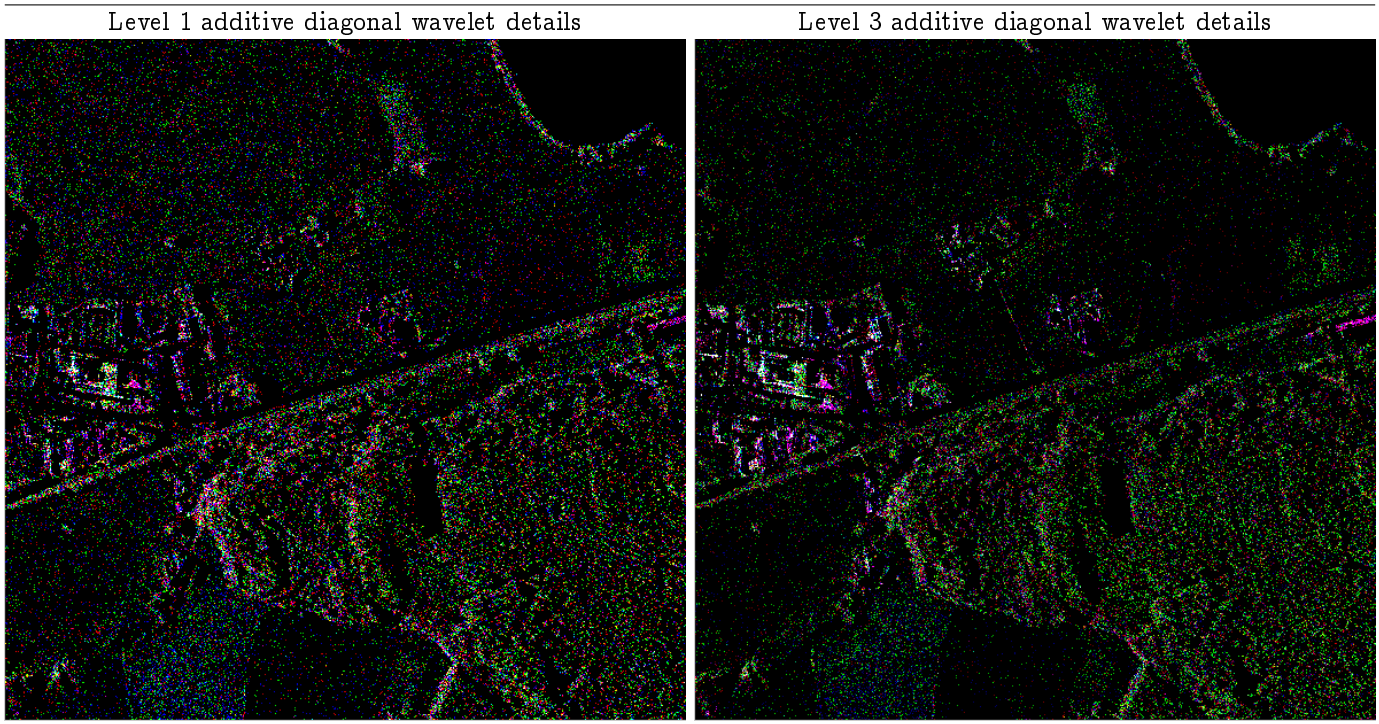


Fig. 2. Detail wavelet coefficients of the image given in Figure 1 when the Haar wavelet is used in an additive wavelet decomposition.

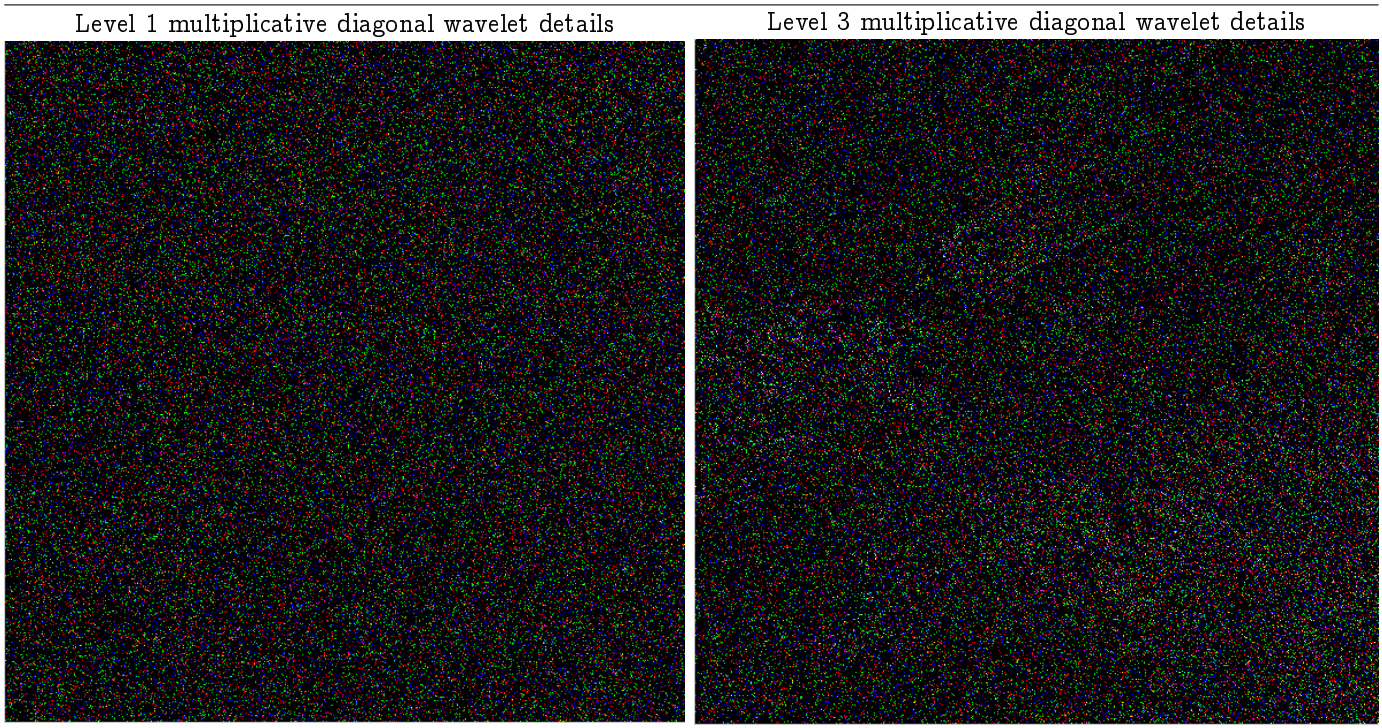


Fig. 3. Detail wavelet coefficients of the image given in Figure 1 when the Haar wavelet is used in an multiplicative wavelet decomposition.